

RSC Pharmaceutics

Accepted Manuscript

This article can be cited before page numbers have been issued, to do this please use: C. Murphy, G. Williamson, L. Ontiveros-Padilla, A. T. Hendricksen, B. T. Johnson-Weaver, H. W. Choi, D. Gooden, S. Kalpathy, A. M. Lopez, E. S. Pena, J. M. Bachelder, R. S. Sellers, S. Abraham, H. Staats and K. Ainslie, *RSC Pharm.*, 2026, DOI: 10.1039/D5PM00380F.



This is an Accepted Manuscript, which has been through the Royal Society of Chemistry peer review process and has been accepted for publication.

Accepted Manuscripts are published online shortly after acceptance, before technical editing, formatting and proof reading. Using this free service, authors can make their results available to the community, in citable form, before we publish the edited article. We will replace this Accepted Manuscript with the edited and formatted Advance Article as soon as it is available.

You can find more information about Accepted Manuscripts in the [Information for Authors](#).

Please note that technical editing may introduce minor changes to the text and/or graphics, which may alter content. The journal's standard [Terms & Conditions](#) and the [Ethical guidelines](#) still apply. In no event shall the Royal Society of Chemistry be held responsible for any errors or omissions in this Accepted Manuscript or any consequences arising from the use of any information it contains.

Dual-Adjuvant Mucosal Vaccine Leveraging Mast Cell and TLR9 Agonists for Protection Against Poxvirus Infection

Connor T. Murphy¹, Grace L. Williamson¹, Luis Ontiveros-Padilla¹, Aaron T. Hendricksen¹, Brandi T. Johnson-Weaver³, Hae Woong Choi³, David M. Gooden⁴, Santhosh Kalpathy⁴, Alexandra M. Lopez¹, Erik S. Pena², Jacob M. Bachelder⁵, Rani S. Sellers⁶, Soman N. Abraham³, Herman F. Staats^{3,7}, Kristy M. Ainslie^{1,2,8*}

¹Division of Pharmacoengineering & Molecular Pharmaceutics, Eshelman School of Pharmacy, UNC, Chapel Hill, NC, USA

²Department of Biomedical Engineering, NC State/UNC, Chapel Hill, NC, USA

³Department of Pathology, Duke University, Durham, NC, US

⁴Department of Chemistry, Duke University, Durham, NC, US

⁵Carborro High School, Chapel Hill, NC, US

⁶Department of Pathology & Laboratory Medicine, School of Medicine, UNC, Chapel Hill, NC

⁷Duke Human Vaccine Institute, Duke University School of Medicine, Durham, NC, USA

⁸Department of Microbiology and Immunology, School of Medicine, UNC, Chapel Hill, NC, USA

*Correspondence:

Kristy M. Ainslie

Fred Eshelman Distinguished Professor

Division of Pharmacoengineering & Molecular Pharmaceutics

UNC Eshelman School of Pharmacy

4012 Marsico Hall, 125 Mason Farm Road

Chapel Hill, NC 27599, United States

ainsliek@email.unc.edu

Keywords: Mast cells, Mast cell activators, mucosal vaccine, adjuvant, Orthopoxvirus,



Abstract

Mast cells (MC) are innate immune cells that are predominantly localized under the skin and at mucosal surfaces, and play a role in numerous physiological processes, including host response to pathogens. Recently, mast cell activators (MCA) have been identified as mucosal vaccine adjuvants that are able to promote a strong and antigen-specific immune response. We performed an extensive structure-activity relationship (SAR) analysis on the previously identified small molecule MCA, ST101036, to further optimize its adjuvanticity. This led to the development of the derivative, VAP-1185, which demonstrated improved mast cell degranulation activity *in vitro*, and a Th2-biased *in vivo* immune response. While mucosal vaccines with a single adjuvant have shown effectiveness, combining two adjuvants can activate multiple immune pathways, leading to a stronger and more comprehensive immune response. Additionally, dual adjuvant vaccines can elicit a balanced Th1/Th2 response, leading to equally effective cellular and humoral responses. We combined VAP-1185 with the FDA-approved adjuvant, cytosine phosphoguanine (CpG), which activates toll-like receptor 9 (TLR9) and promotes a Th1-biased immune response. This dual adjuvant formulation promotes inflammatory cytokine production *in vitro*, additive humoral effects and an active cellular response *in vivo*, as well as a favorable safety profile when intranasally administered to C57BL/6 mice. Subsequently, this adjuvant formulation was also able to confer protection against a lethal challenge of vaccinia virus in BALB/c mice. Thus, we report a novel mucosal vaccine formulation that produces an effective Th1/Th2 balanced immune response.



Introduction

The genus, *Orthopoxvirus*, is characterized as a group of brick-shaped, double-stranded DNA viruses that possess very low mutation rates. Some of the most clinically relevant orthopoxviruses include smallpox, mpox (formerly monkeypox), cowpox, and vaccinia virus. Due to the highly conserved antigenic similarities between each virus, infection with one orthopoxvirus will generate cross-reactive immunity against others.¹ One of the most well-known orthopoxviruses, smallpox is widely considered one of the deadliest human diseases to ever exist, with an estimated 300-500 million deaths attributed to smallpox in just the 20th century alone. Fortunately, due to a World Health Organization (WHO) led mass vaccination campaign, smallpox was declared officially eradicated in 1980.² However, despite its eradication, smallpox is still a major concern due to the gradual decline in global immunity, the threat of bioterrorism, and the emergence of related orthopoxviruses, as demonstrated by the recent global increase in mpox epidemics.^{3, 4} Currently, there are two FDA-approved vaccines available for orthopoxviruses: ACAM2000® and JYNNEOS®. ACAM2000® utilizes a live, replication-competent strain of vaccinia virus to stimulate a highly potent immune response. However, due to the vaccinia virus's ability to replicate, ACAM2000® cannot be administered to special populations who are immunocompromised, such as infants, the elderly, pregnant women, those with autoimmune diseases or those with cancer, as there is a risk that they could become sickened by the virus. Alternatively, JYNNEOS® also utilizes live vaccinia virus, although it is replication-incompetent, making it much safer for immunocompromised populations to receive.⁵ Unfortunately, the long-term protective immunity induced by JYNNEOS® is of concern, as a recent study found that neutralizing antibodies generated by the vaccine quickly decline 6-12 months post vaccination.⁶



Therefore, an orthopoxvirus vaccine that is highly effective, yet safe for immunocompromised populations to receive is desperately needed.

Both available orthopoxvirus vaccines and most WHO-approved vaccines require needles, providing disadvantages such as painful administration, the generation of biohazardous waste, and a lack of IgA antibody production which is beneficial for preventing infection at mucosal sites.⁷ Intranasal (I.N.) mucosal vaccines are a promising alternative, as they are painless, easily administered, and promote systemic IgG antibody production as well as IgA at the site of administration and at distant mucosal surfaces.⁸ Considering that the vast majority of clinically relevant pathogens enter the body through mucosal sites (e.g., gastrointestinal, nasopharyngeal, respiratory, and genitourinary tracts), including smallpox and mpox, the presence of antigen-specific IgA antibodies is crucial for providing protection at the source of pathogen entry.^{9, 10} However, mucosal barriers are often highly immunotolerant due to the constant exposure to a wide assortment of environmental and food-borne antigens. Therefore, mucosal vaccine formulations benefit from the inclusion of adjuvants to stimulate an effective immune response.¹¹ Unfortunately, the development and widespread implementation of mucosal vaccines is currently hampered by a lack of safe and effective adjuvants for this route of administration. Although there are a wide assortment of mucosal vaccine adjuvants available for use in pre-clinical studies, most are either not approved for or not considered safe for use in humans.¹² Therefore, the development of new adjuvants is paramount for furthering the development of mucosal vaccines.

Mast cell activators (MCAs) are a novel class of vaccine adjuvants that can act as effective mucosal vaccine adjuvants, while maintaining an acceptable safety profile.¹³



Mast cells (MCs) are a specialized type of granulocyte of the innate immune system that are distributed throughout the body, but are prevalent in and around mucosal surfaces, as well as under the skin. They are one of the primary cell types associated with allergic reactions and anaphylaxis, yet, MCs also play a role in a multitude of physiological responses, including pathogen detection and response.¹⁴ Upon interacting with a pathogen, MCs become activated and undergo a process called degranulation, where pre-formed granules release immunostimulatory mediators, such as inflammatory cytokines, into circulation which promotes the downstream activation of other immune cell types and the initiation of an immune response.¹⁵ By utilizing MCAs to induce the localized degranulation of MCs, a highly-specific and potent immune response can be developed if antigen is present, ideal for vaccines. We have previously reported the identification of 15 small molecule MCAs through a high-throughput screen of over 55,000 compounds.¹⁶ Of the 15 molecules, the compound, ST101036, was found to induce a substantial *in vivo* immune response when encapsulated in acetalated dextran (Ace-DEX) microparticles (MPs).¹⁷ Based on these results, we selected ST101036 for further optimization via structure-activity relationship (SAR) analysis evaluating MC degranulation.

Given its classification as an MCA, our new small-molecule adjuvant is predicted to drive a Th2-skewed immune responses mostly through driving differentiation via the antigen presenting cells (e.g. dendritic cell) and T cell synapse.¹⁸ While Th2-biased responses are associated with a greater humoral immunity, utilizing a dual-adjuvant strategy to also stimulate an enhanced Th1-biased cellular response can lead to more robust and comprehensive immune activation. To achieve an effective Th1/Th2 balanced mucosal vaccine formulation, we combined VAP-1185 with the mouse version of the FDA-



approved, synthetic oligonucleotide, cytosine phosphoguanine (CpG), a potent toll-like receptor 9 (TLR9) agonist that is known to have a Th1-bias.¹⁹ We evaluated a intranasally administered mucosal vaccine that paired a newly identified small molecule MCA with CpG with antigens, ovalbumin (OVA) or vaccinia virus protein B5R. These vaccination formulations were evaluated for humoral and cellular responses as well as survival after a lethal vaccinia virus challenge.

Materials and Methods

All chemicals were purchased from Sigma (St. Louis, MO) and used as purchased unless otherwise specified. CpG ODN 1826 was obtained from Invivogen (San Diego, CA). Assays and disposables were sourced from Thermo Fisher Scientific (Waltham, MA) unless indicated otherwise. VAP-1185 was synthesized by the Duke Small Molecule Synthesis Facility (SMSF; Duke University, Durham, NC). The following reagent was obtained through the NIH Biodefense and Emerging Infections Research Resources Repository (BEI), NIAID, NIH: vaccinia virus (WR) B5R protein with N-terminal histidine tag, recombinant from baculovirus, NR-546.

MC/9 cell culture and degranulation assay

MC/9 cells (ATCC, Manassas, VA) were cultured in DMEM containing 4 mM L-glutamine, 4.5 g/L glucose, and 1.5 g/L sodium bicarbonate. Media was supplemented with 10% fetal bovine serum (FBS), 10% rat T-STIM, 2mM L-glutamine, 0.05 mM 2-mercaptoethanol and 1% penicillin/streptomycin (P/S) and maintained in a 37 °C incubator with 5% CO₂ and ≥95% relative humidity. MC/9 cells were washed 2x in Tyrode's buffer (3.94 g NaCl, 0.19 g KCl, 0.1 g CaCl₂, 0.05 g anhydrous MgCl₂, 0.5 g



glucose, 6.7 mL bovine albumin fraction V (7.5%), 10 mL HEPES (1M) and distilled water to 500 mL) and seeded in a tissue culture treated 96-well U-bottom plate at 1×10^5 cells/well. The cells were treated with the compounds and left to incubate for 30 minutes at 37 °C. Tyrode's buffer alone was used as a negative control, and 0.1% Triton-X100 was used as a positive control. After 30 minutes, the plate was centrifuged at 450 x g for 5 minutes and 30 μ L of supernatant was removed and mixed with 10 μ L of p-nitrophenyl-N-acetyl- β -D-glucosaminide (NAG) substrate made in 0.1 M citrate buffer (pH 4.5) in a separate 96-well U-bottom plate and left to incubate for 1 hour at 37 °C. After the incubation, carbonate buffer (pH 10) was added, and the absorbance was measured at 405 nm. Percent degranulation was calculated using the following formula:

$$\text{Percent degranulation (\%)} = 100 \times \frac{(\text{Experimental release} - \text{Tyrode's release})}{(\text{Triton} - \text{X100 release} - \text{Tyrode's release})}$$

Primary dendritic cell culture and assays

Bone marrow-derived dendritic cells (BMDCs) were prepared in accordance with an established protocol.²⁰ Briefly, marrow was isolated from the femurs and tibias of female C57BL/6 mice and cultured in RPMI-1640 containing L-glutamine and supplemented with 25 mM HEPES, 10% FBS, and 1% P/S (base media). Every 2 days for 14 days, half the volume of the media was discarded and replaced with fresh base media supplemented with 10 ng/mL of murine GM-CSF. On the last 4 days of culture, cells received base media supplemented with GM-CSF and 10 ng/mL of murine IL-4 (PeproTech®). Cells were cultured in a 37°C incubator with 5% CO₂ and $\geq 95\%$ relative humidity. BMDCs (2.5×10^4 cells/well) were seeded in a tissue culture treated 96-well plate and left to adhere overnight. The following day, the cells were treated with the individual



adjuvants alone, and in combination with one another and left to incubate for 48 hours. After 48 hours, the plate was centrifuged at 350 x g for 5 minutes and the supernatants were removed. The production of lactate dehydrogenase (LDH) was measured according to the manufacturer's protocol (CyQUANT™ LDH Cytotoxicity Assay Kit, Invitrogen, Waltham, MA). Quantified LDH was normalized to a maximum LDH positive control (10X Lysis Buffer) and a negative control (no treatment – media). To assess inflammatory cytokine production, ELISAs were performed according to the manufacturer's protocol for quantifying the production of TNF- α and IL-6 (BioLegend, San Diego, CA).

SAR Analysis

SAR analysis focused on three key sites of modification to the pyrimidine core of ST101036: (1) the R₁ position, where chiral methyl piperazine derivatives were introduced with improved solubility; (2) the R₂ position, modified with 4'-phenyl alkyl groups; and (3) the addition of a trifluoromethyl (CF₃) group, which was found to be critical for degranulation activity. Analogs were evaluated by the following criteria: (1) high degranulation activity in both mouse (MC/9) and human (LAD2) cell lines, (2) analogs/derivatives that are able to be easily synthesized in few steps, and (3) analogs with appropriate molecular diversity. Among the analogs evaluated, VAP-1185 was identified as the lead MCA based on these criteria.

SAR analysis utilized a site-directed modification strategy that focused on the pyrimidine core of ST101036, targeting the 2-amino group (R₁) and the 4'-substituent (R₂) of the aryl moiety. At the R₁ position, the 2-amino group was replaced with various chiral methyl piperazine derivatives, while the R₂ position 4-aryl group was replaced with a variety of



substituted aryl and alkyl-aryl groups.

^1H and ^{13}C Nuclear Magnetic Resonance (NMR)

Structural characterization of VAP-1185 was performed on a Bruker AVANCE NEO 500 MHz spectrometer located at the University of North Carolina NMR Core Facility. High-sensitivity data acquisition was facilitated by a 5 mm Prodigy CryoProbe equipped with an automated tuning and matching (ATM) unit and a pulsed-field gradient (PFG) accessory. All spectra were acquired in CDCl_3 at 298 K. ^1H NMR spectra were recorded at 500 MHz and referenced to residual CDCl_3 ($\delta 7.26$ ppm). ^{13}C NMR spectra were recorded at 125 MHz with simultaneous broadband ^1H -decoupling and referenced to the center line of the CDCl_3 triplet ($\delta 77.16$ ppm). CDCl_3 was purchased from Cambridge Isotope Laboratories (Tewksbury, MA). All NMR spectra were analyzed using MestreNova software (Version 15.0.1)

Mass Spectrometry

VAP-1185 was analyzed with a Q Exactive HF-X (ThermoFisher, Bremen, Germany) mass spectrometer. Samples were introduced via a heated electrospray source (HESI) at a flow rate of 10 $\mu\text{L}/\text{min}$. At least thirty time domain transients were averaged in the mass spectrum. HESI source conditions were set as: nebulizer temperature 100 deg C, sheath gas (nitrogen) 15 arb, auxiliary gas (nitrogen) 5 arb, sweep gas (nitrogen) 0 arb, capillary temperature 250 degrees C, RF voltage 100 V. The mass range was set to 600-2000 m/z. All measurements were recorded at a resolution setting of 120,000. Solutions were analyzed at 0.1 mg/mL or less based on



responsiveness to the ESI mechanism. Xcalibur (ThermoFisher, Bremen, Germany) was used to analyze the data. Molecular formula assignments were determined with Molecular Formula Calculator (v 1.3.0). All observed species were singly charged, as verified by unit m/z separation between mass spectral peaks corresponding to the ^{12}C and ^{13}C isotopes for each elemental composition.

Transepithelial Electrical Resistance (TEER) analysis

Human nasal epithelial RPMI 2650 cells (ATCC) were cultured in DMEM supplemented with 10% FBS and 1% P/S and then seeded at 2×10^6 cells/well in 6-well transwell inserts and cultured for two days in a 37 °C incubator with 5% CO_2 and $\geq 95\%$ relative humidity to form visible tight junctions. We used the TEER device that was described previously.²¹ Prior to TEER measurement cells were treated with 1.25 $\mu\text{g}/\text{ml}$ of VAP-1185. Background of blank wells without cells were subtracted from each measurement. As is convention, the resistance measured is multiplied by the surface area of the transwell ($\Omega \cdot \text{cm}^2$) and then we normalized by time zero.²² For a six well transwell, the surface area is 4.67 cm^2 according to the manufacturer's website.

Immunization

For formulation, VAP-1185 was solubilized in PEG400 (Sigma Aldrich), CpG and EndoFit™ OVA protein (Invivogen) were both solubilized in sterile PBS, and each component was combined in equal volumes and gently pipetted to mix. Only the VAP-1185 alone, and VAP-1185/CpG group contained PEG400 in the formulation. A limulus amoebocyte lysate (LAL) endotoxin quantification assay (Thermo Fisher Scientific) was



performed to quantify the presence of endotoxin in the PEG400. The PEG400 was found to possess undetectable levels of endotoxin (<0.1 EU/mL). Both CpG and the EndoFit™ OVA protein were free of endotoxin. 6-8-week-old, female, C57BL/6J and BALB/c mice were purchased from Jackson Laboratory (Bar Harbor, ME). Groups of 10 female C57BL/6 mice were intranasally (I.N.) administered either PBS, OVA (10 µg) in PBS, VAP-1185 (18 µg) + OVA (10 µg), CpG (2 µg) + OVA (10 µg), or VAP-1185 (18 µg) + CpG (2 µg) + OVA (10 µg). Mice received 7.5 µL in each nare (15 µL total) under isoflurane anesthesia on days 0, 21, and 35. Blood for serology was collected into MiniCollect® CAT Serum Separator Tubes from the submandibular vein on days 14, 28, 42, and 56. Blood was centrifuged for 10 minutes at 3,000 x g and the isolated serum was stored at -80 °C until use.

On day 63, mice were humanely euthanized, at which time bronchoalveolar lavage (BAL) and a nasal wash (NW) were performed and spleen was collected. BAL and NW samples (1 mL each) were stored at -80 °C until evaluation. Lavage wash was prepared by combining PBS with 0.01% Triton X-100 with protease inhibitor cocktail tablets (1 tablet per 20 mL of lavage fluid). For BAL collection, a 22G x 1" catheter was inserted into the trachea of the mouse, and the lungs were flushed three times with 1 mL of lavage fluid. To collect nasal washes, the same catheter was reinserted into the trachea and lavage fluid was flushed through the nasal passages and collected in sterile 1.5 mL microcentrifuge tubes. Spleens were mechanically dissociated into single-cell suspensions for use in ELISpot assay.²³

Antibody titers



Flat bottom 384-well plates (Greiner Bio-One, Austria) were coated with 5 $\mu\text{g}/\text{mL}$ of OVA protein (Worthington Biochemical Corp., Lakewood, NJ) in PBS and incubated at 4 $^{\circ}\text{C}$ overnight. The next day, the plates were washed 3x with wash buffer (PBS with 0.05% Tween-20) using a plate washer (Biotek ELX405, Agilent, Santa Clara, CA) and blocked for 1 hour with blocking buffer (3% non-fat instant milk in PBS) at room temperature (RT). The plates were washed 3x with wash buffer and a 1:100 dilution of serum samples were serially diluted 5-fold and incubated for 2 hours at RT. A 1:10 dilution of both BAL and NW samples was performed prior to titration. The plates were washed 3x with wash buffer and isotype-specific secondary antibodies (goat anti-mouse IgG, goat anti-mouse IgG1, goat anti-mouse IgG2c, goat anti-mouse IgG2a, goat anti-mouse IgA (Southern Biotech, Birmingham, AL)) were diluted in blocking buffer and added to the plates to incubate for 30 minutes at RT. The plates were washed 5x with wash buffer and tetramethylbenzidine (TMB) one-component substrate (Southern Biotech) was added to each well and left to incubate until a colorimetric gradient developed. The reaction was quenched with 2 N sulfuric acid, and the absorbance was read on a plate reader at 450 nm and 570 nm (Spectramax M2, Molecular Devices, San Jose, CA).

ELISpot

MultiScreen-IP 0.45- μm filter 96-well plates (Sigma-Aldrich) were pre-wet with 70% ethanol for 1 minute and washed with PBS before being coated with anti-mouse IFN- γ or anti-mouse IL-2 capture antibody in PBS (BD, Franklin Lakes, NJ) and left to incubate at 4 $^{\circ}\text{C}$ overnight. The following day, the capture antibody was aspirated, and the wells were blocked with cell culture medium (RPMI 1640 w/ L-glutamine and supplemented



with 10% FBS and 1% P/S) for 2 hours at RT. The cell culture medium was removed and 1×10^6 splenocytes was added to each well and stimulated with either 10 $\mu\text{g}/\text{mL}$ of vaccine-grade OVA or OVA peptide, SIINFEKL (AnaSpec, Fremont, CA) in cell culture media and placed in a 37 °C incubator with 5% CO_2 and $\geq 95\%$ relative humidity for 36 hours. The plate was washed 2x with deionized water and left to soak for 5 minutes during each wash. Plates were then washed 3x with wash buffer and anti-IFN- γ and anti-IL-2 detector antibodies were diluted in dilution buffer (PBS with 10% FBS) and left to incubate for 2 hours at RT. The detection antibodies were aspirated, and wells were washed 3x with wash buffer and streptavidin-HRP (BD) in dilution buffer was added to each well and incubated for 1 hour at RT. The streptavidin-HRP was aspirated, and wells were washed 5x with wash buffer, followed by being washed 2x with PBS. AEC substrate solution (BD) was added to each well until spots were detectable. The reaction was quenched by the addition of deionized water. Plates were dried for 48 hours at RT and spots were counted using an ImmunoSpot plate reader (CTL).

Viral Challenge

6-8-week-old, female, BALB/c mice were divided into 5 groups of 10 mice per group and I.N. vaccinated on the same schedule described previously, with BR5 protein (BEI Resources, Manassas, VA) in place of OVA. BALB/c mice were used rather than C57BL/6 mice, as BALB/c mice are more susceptible to vaccinia virus infection. Animals were administered either PBS, VAP-1185 (18 μg) + B5R (10 μg), CpG (2 μg) + B5R (10 μg), VAP-1185 (18 μg) + CpG (2 μg) + B5R (10 μg), or AddaVax™ (Invivogen) + B5R (10 μg) (1:1 solution intramuscularly). AddaVax™, a squalene-based oil-in-water emulsion



that mimics the FDA-approved adjuvant, MF59, was formulated with the B5R protein and administered intramuscularly as a positive control. On day 56, mice were anesthetized with isoflurane and I.N. challenged with 5×10^4 PFU of Vaccinia Virus – Western Reserve (25 μ L/nare) (BEI Resources). Body weight and clinical scores were measured daily for 14 days after viral challenge, and mice that lost 20% of their original body weight were humanely euthanized.

Neutralizing antibodies

Six grams of carboxymethylcellulose sodium, medium viscosity, was combined with distilled water and heated on a stir plate until completely dissolved to form a 3% carboxymethylcellulose (CMC) matrix. The CMC matrix was autoclaved at 121 °C for 30 minutes. The liquid overlay diluent (LOD) was made by supplementing 500 mL of MEM 2X, without phenol red with 40 mL of FBS, 10 mL of 200 mM L-glutamine, 10 mL of 100X non-essential amino acids, 7.5 mL of 100X sodium bicarbonate solution (7.5%) and sterile filtered. BS-C-1 cells (ATCC) were cultured in MEM (1X) and supplemented with 10% FBS and 1% P/S. Cells were plated in tissue culture treated 12-well plates at 3.75×10^5 cells/well and left to adhere overnight in a 37 °C incubator with 5% CO₂ and $\geq 95\%$ relative humidity. Serum samples were heat-inactivated by placing in a 56 °C water bath for 30 minutes and then cooled on ice for 5 minutes. Heat-inactivated serum samples were diluted 1:10 in MEM (1X) with 2.5% FBS and 1% P/S and combined with a 1:50,000 dilution of vaccinia virus – Western reserve at equal volumes 1:1 and placed in a 37 °C incubator for 1 hour to allow for neutralization to occur. A 1:100,000 dilution of virus alone was used as the virus control and virus combined 1:1 with a 1:25 dilution of a polyclonal



rabbit anti-vaccinia virus antibody (Tetracore, Inc., Rockville, MD,) as a positive control for neutralization. Media was aspirated from the cells and 210 μ L of each sample was plated and left to incubate for 2 hours at 37°C. The CMC matrix and LOD were combined in equal volumes and placed in a 37 °C water bath for at least 30 minutes. After the incubation, 1.5 mL of the CMC/LOD was added and the plate was left to incubate at 37 °C for 48 hours. After the incubation, the overlay was aspirated, wells were washed with warmed 1X PBS, and 250 μ L of 0.1% crystal violet in 20% ethanol was added to each well and left to incubate for 30 minutes at room temperature. The crystal violet was aspirated, and plaques were enumerated.

Histology and blood chemistry

Acute local tolerance was assessed in C57BL/6 female mice, where mice were administered PBS, VAP-1185, CpG, or VAP-185 and CpG as indicated above, with OVA as antigen. Mice (3 per group) were administered test material in each nare as indicated above under isoflurane anesthesia, allowed to recover, and humanely euthanized 24 h after administration. Blood for serum chemistry was collected by submandibular bleed as described previously. Nose and calvarium were fixed in 10% neutral-buffered formalin for several days and decalcified in Immunocal® (StatLab Medical Products, Inc., McKinney, TX,) for 48 hours. Tissues were then trimmed into four sections encompassing the following regions: (1) posterior portion of the upper incisors, (2) incisive papilla, (3) second palatine crest, and (4) first molar teeth. Samples were routinely processed, paraffin-embedded, sectioned at 5 μ m, and stained with hematoxylin and eosin in the Pathology Services Core Facility at the University of North Carolina at Chapel Hill. A board-certified veterinary pathologist evaluated all slides using a qualitative scoring system for



microscopic findings: 0 = no findings; 1 = minimal; 2 = mild; 3 = moderate; 4 = marked; 5 = severe. Serum levels of alanine transaminase (ALT) were measured by the Animal Clinical Chemistry Core at UNC from mice 24 hours after vaccination.

Ethics

All animal experiments were performed in accordance with the guidelines of the University of North Carolina at Chapel Hill and approved by the Institutional Animal Care and Use Committee (IACUC).

Statistics

All data and statistical analysis were performed using GraphPad Prism 10.5.0. One-way ANOVAs with Tukey's multiple comparisons were performed for all *in vitro* assays and both One- and Two-way ANOVAs with Tukey's multiple comparisons were performed for *in vivo* analysis.

Results & Discussion

VAP-1185 was identified as a potent analog of ST101036.

Based on previously observed results, ST101036 was chosen for further optimization due to its degranulation activity *in vitro* and *in vivo* immune response.¹⁷ Three primary modifications were proposed for optimization of ST101036 (**Figure 1A**). Initial SAR of the pyrimidine core was achieved through modification of the 2-amino group (R₁) and modification of the 4'-substituent (R₂) on the 4-aryl group (**Figure 1B**). This approach produced a library of 35 new derivatives (**Supplementary Table 1**). Of these derivatives, VAP-1185 was identified as the most potent MCA with improved degranulation activity compared to parent compound ST101036 (**Figure 1C & D & Supplementary Figures 1-**



3). This aspect of the SAR analysis showed that alkyl-amino groups are incompatible with activity, while replacement of amino piperidine to chiral 2-methyl amino piperazine improved activity. Modification of the R₂ position with various alkyl groups was well tolerated. Notably, replacement of the CF₃ group with a methyl group abolished all activity, indicating that the inductive effects of the CF₃ group are required for biological effect.

While specific ligand-receptor interactions between VAP-1185 and MCs is currently unknown, classical MC degranulation occurs through multivalent cross-linking of IgE-bound FcεRI receptors. However, other receptors such as Mas-related G protein-coupled receptor member X2 (MGRPRX2) can also induce degranulation independently of IgE.²⁴ This suggests that VAP-1185 may activate mast cells through a non-IgE-mediated mechanism. One method of adjuvant activity could be the result of decreased tight junctions in mucosal epithelium.²⁵ To assess this, the transepithelial electrical resistance (TEER) of VAP-1185 was measured using a TEER meter and RPMI 2650 cells, derived from the nasal septum of a male patient with squamous cell carcinoma.²⁶ After 30 minutes, there was no decrease in integrity of tight junctions of the RPMI 2650 cells (**Supplementary Figure 4**). It has been shown that the MCA, Compound 48/80, when added to tight junctions does not significantly alter the resistance measured by TEER.²⁷ Therefore, it appears that VAP-1185 does not boost the immune response by disrupting tight junctions present in the nasal passage. The mechanism underlying VAP-1185 MC activation remains to be elucidated, but its potential adjuvanticity warrants further *in vitro* investigation.



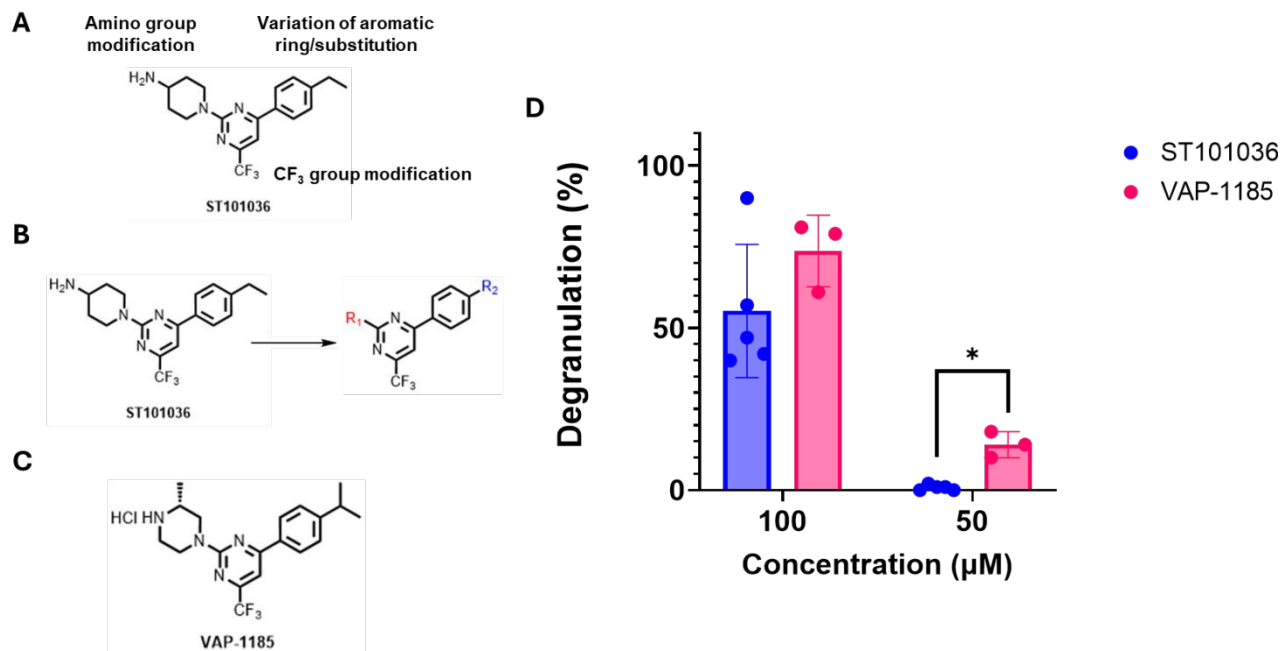


Figure 1. SAR analysis and *in vitro* mast cell degranulation activity of ST101036 and VAP-1185. (A) Proposed SAR analysis of ST101036. (B) General schematic of lead candidate SAR modification sites. (C) Lead analog VAP-1185 of parent compound, ST101036. (D) MC/9 cell degranulation after stimulation with ST101036 and VAP-1185. Significant differences determined by using a Mann-Whitney test (* $p \leq 0.05$).

VAP-1185 combined with CpG induces an inflammatory cytokine response *in vitro*

To assess the ability of the adjuvant combination to effectively activate innate immune cells, we stimulated BMDCs with VAP-1185 alone, CpG alone, and then a combination of the two. The subsequent cell viability was measured, and the production of pro-inflammatory cytokines was quantified. VAP-1185 induced significant toxicity at 1 µg while CpG was found to be non-toxic at the evaluated dose. When combined, the adjuvants were not cytotoxic (**Figure 2A**). While we expected MCA VAP-1185 to induce a Th2-biased immune response *in vivo*, it produced very little of either IL-6 (a Th2-associated cytokine) or TNF-α (a Th1-associated cytokine), whereas CpG increased production of both. In combination, the two adjuvants produced moderate amounts of IL-6 and TNF-α, with the addition of VAP-1185 reducing the overall cytokine response



induced by CpG alone (**Figure 2B & C**). Further studies will examine additional cytokines and innate immune cell populations to determine the additional effects of these adjuvants in combination.

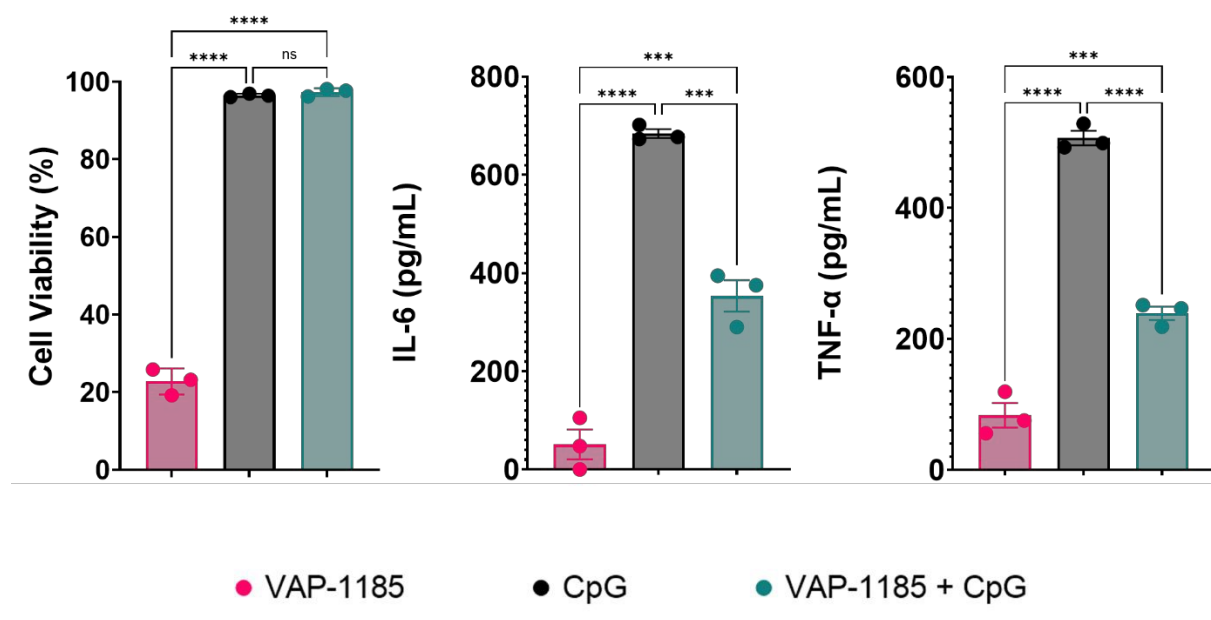


Figure 2. BMDCs were stimulated with either VAP-1185 alone (1 μ g), CpG alone (1 μ g), or VAP-1185 and CpG in combination (0.63 μ g/1 μ g) for 48 hours. (A) The presence of LDH was measured as a marker for cell viability and the production of (B) IL-6 and (C) TNF- α were measured as markers for inflammatory cytokine production. Data presented as mean + standard error of the mean. Significant differences determined by using a two-way ANOVA with Tukey's multiple comparisons (ns = not significant; * $p \leq 0.05$; **** $p < 0.001$).

VAP-1185 combined with CpG induces additive humoral effects *in vivo*.

VAP-1185 and CpG were combined with OVA and intranasally administered to C57BL/6 mice on days 0, 21, and 35 on a prime-boost-boost schedule (n=5). By day 56, mice that received VAP-1185 and CpG in combination produced IgG titers that were significantly greater than those produced by mice that received either adjuvant individually

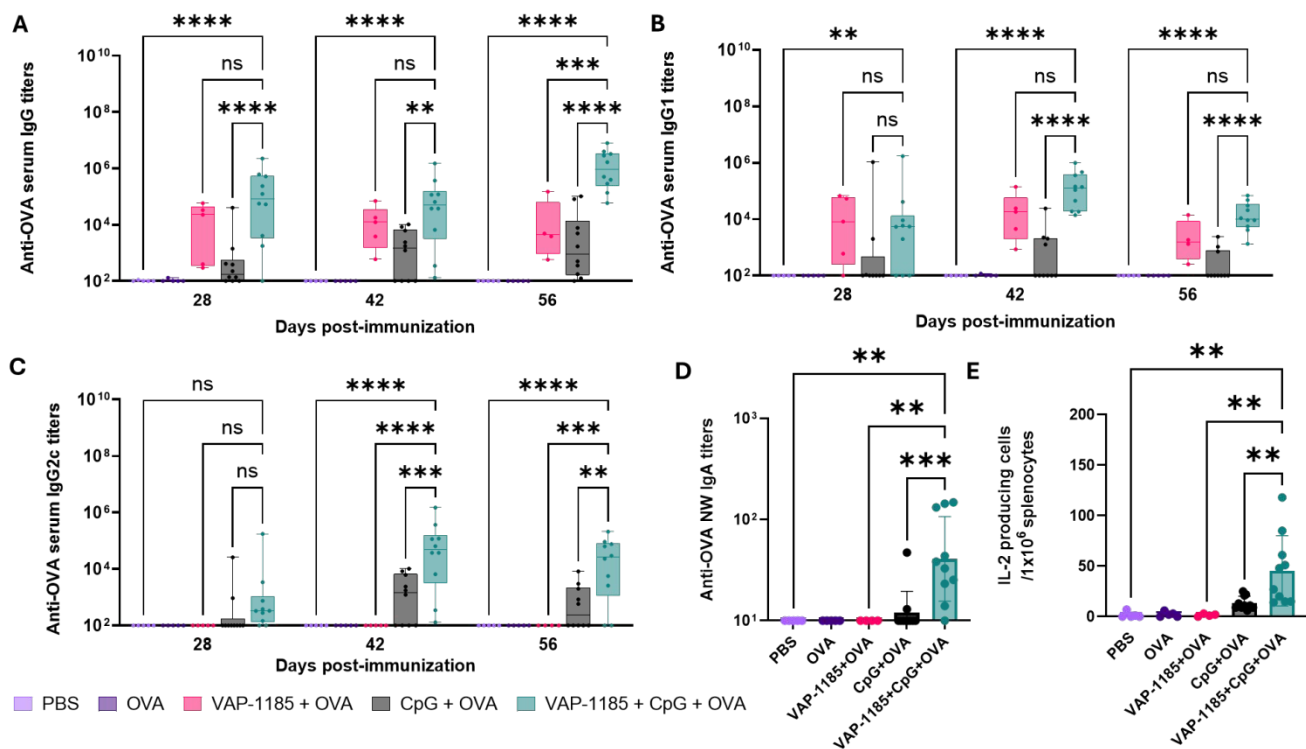


(Figure 3A). One mouse in the VAP-1185 group alone died following the submandibular bleed on day 42. IgG1 titers, which are associated with a Th2-biased response, peaked on day 42 and gradually decreased by day 56. The combination group produced IgG1 titers that were greater than CpG, yet not statistically different than VAP-1185 alone **(Figure 3B)**. IgG2c titers, which are associated with an Th1-biased response, were also significantly greater than either adjuvant alone **(Figure 3C)**. The lack of an IgG2c response from VAP-1185 further demonstrated that VAP-1185 is a Th2-biased adjuvant as this is typically a Th1 skewed antibody for C57BL/6 mice.²⁸. Importantly, the adjuvant combination produced additive total IgG titers and enhanced both Th1-associated (IgG2c) and Th2-associated (IgG1) antibody responses, matching or exceeding the levels elicited by each adjuvant alone.

To assess the production of antigen-specific antibodies in mucosal tissues, mice received an additional vaccine boost on day 56 and were sacrificed on day 63 for bronchoalveolar lavage (BAL) and nasal wash (NW) collection. OVA-specific IgA titers in the NW of the combined adjuvant group were significantly higher than those generated by either adjuvant alone. **(Figure 3D)**. The increased antigen-specific IgA in the nasal canal following I.N. immunization with OVA formulated with both adjuvants highlights the advantage of this dual-adjuvant approach. No significant differences were observed between the combination and individual adjuvants for NW IgG, with the exception that NW IgG titers were significantly higher than those produced by CpG alone **(Supplementary Figure 5)**.



To evaluate the antigen-specific cellular immune responses induced by the different vaccine formulations, splenocytes were harvested on day 63 and stimulated with either the complete OVA protein used in the vaccine, or with the OVA MHC I immunodominant peptide, SIINFEKL. Splenocytes from both the CpG and combination groups produced IL-2 and IFN- γ when stimulated with either full-length OVA or the SIINFEKL peptide (**Supplementary Figure 6**). Overall, cytokine levels did not differ significantly between the two groups, except for IL-2 production in response to SIINFEKL, where the combination group generated significantly higher IL-2 than the CpG and VAP-1185 alone group (**Figure 3E**). This indicates a stronger CD8⁺ T-cell response elicited by



the combination formulation.

Figure 3. C57BL/6 mice were vaccinated with either PBS, OVA, or OVA combined with each adjuvant individually, and a combination of the two adjuvants on days 0, 21, and 35. OVA-specific serum (A) IgG, (B) IgG1, and (C) IgG2c antibody responses were measured on days 28, 42, and 56. (D) OVA-specific NW IgA antibody responses were measured on day 63. (E) IL-2 production from splenocytes stimulated with SIINFEKL peptide. Data



presented as mean \pm range. Significant differences determined by using a two-way ANOVA for figures A-C, and a one-way ANOVA for figure D with Tukey's multiple comparisons (ns = not significant; * $p \leq 0.05$; ** $p \leq 0.01$; *** $p \leq 0.001$; **** $p \leq 0.001$).

VAP-1185 combined with CpG provides protection in a lethal challenge model

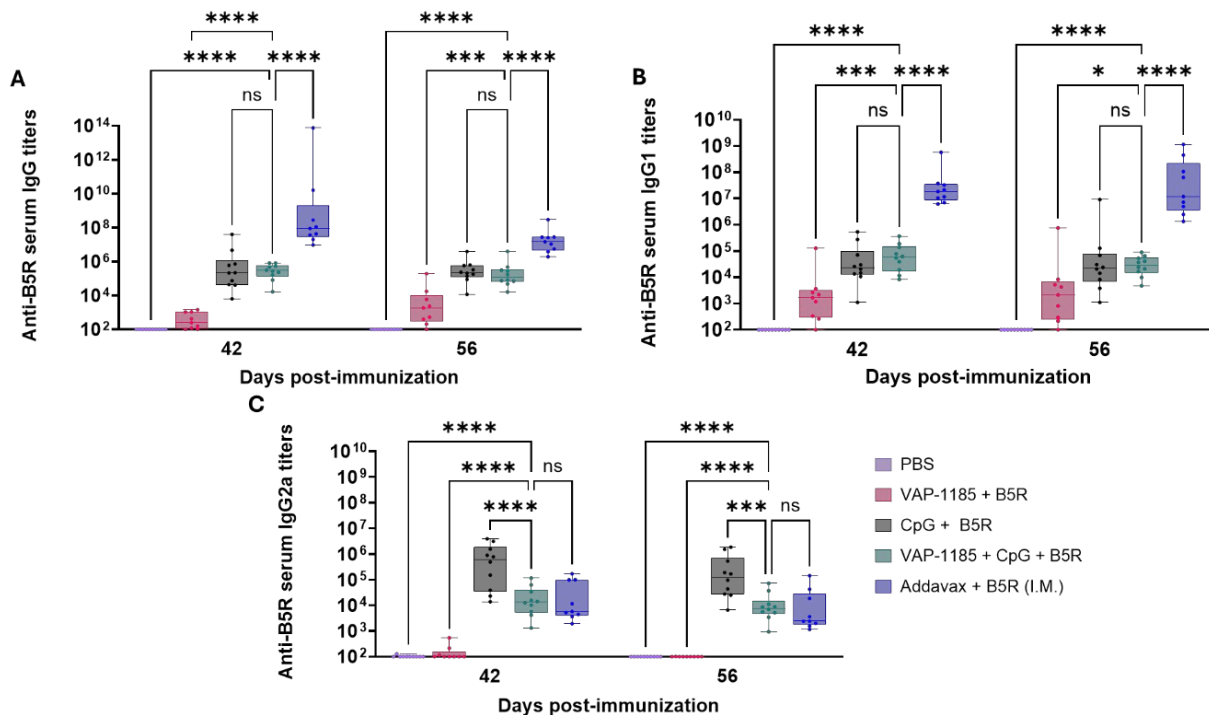
After characterizing the immune response, the protective efficacy of the dual-adjuvant formulation was evaluated using a lethal challenge of vaccinia virus. As previously discussed, vaccinia virus is a member of the genus, *Orthopoxvirus*, and due to its similarity to the more deadly smallpox, vaccinia virus serves as an effective, yet safer surrogate for the infection.²⁹ The protein, B5R, is a vaccinia extracellular envelope virus (EEV) protein that is highly conserved across clinically relevant orthopoxviruses, and is also the primary target of neutralizing antibodies, making it an ideal antigen for use with the formulations.³⁰

The additive effects that had been previously observed when VAP-1185 and CpG were combined with OVA in C57BL/6 mice were reduced when B5R antigen was used in BALB/c mice. Prior to day 42, one mouse in the AddaVax group (n=9) was found dead following a wellness check due to an unknown reason. One mouse in the VAP-1185 group died following the day 56 bleed but prior to challenge (n=9). Vaccine formulations containing CpG alone or CpG combined with VAP-1185 elicited comparable B5R-specific IgG and IgG1 titers at days 42 and 56. In contrast, B5R formulated with VAP-1185 alone induced significantly lower IgG and IgG1 titers than either the CpG or combination groups (**Figure 4A & B**). However, the most notable difference was between CpG and the combination group when evaluating the production of B5R-specific IgG2a antibodies. Previously with OVA, the combination group was producing greater quantities of antigen-specific IgG2c than CpG, yet the opposite was observed with B5R. However, the



combination group was comparable to the positive control AddaVax group, while the VAP-1185 formulation did not produce measurable titers (**Figure 4C**). Variable explanations are possible for differences observed between the antigen-specific antibody responses in the OVA and B5R vaccine groups, although the most likely explanation is due to inherent biological differences between the mouse strains. C57BL/6 mice (vaccinated against OVA) are known to generate predominately Th1-biased immune responses, while BALB/c mice (vaccinated against B5R) have been found to produce Th2-biased responses.³¹

Figure 4. BALB/c mice were vaccinated with either PBS, or B5R with each adjuvant



individually, a combination of the two adjuvants, and Addavax on days 0, 21, and 35. B5R-specific (A) IgG, (B) IgG1, and (C) IgG2a antibody responses were measured on days 42 and 56. Data presented as mean \pm range. Significant differences determined by using a two-way ANOVA with Tukey's multiple comparisons (ns = not significant; * $p \leq 0.05$; ** $p \leq 0.01$; *** $p \leq 0.001$; **** $p \leq 0.0001$).

On day 56, mice were intranasally challenged with a lethal dose of vaccinia virus – Western reserve to assess the protective efficacy of the vaccine formulations. Daily body weight and clinical scores were measured for each group (**Figure 5A & B**). By day



6, all of the PBS group (0% protection), as well as all but one mouse from the VAP-1185 group (11.1% protection), and one mouse from the combination group had succumbed to infection, while all mice in the CpG and AddaVax formulation groups illustrated 100% protection (**Figure 5C**). The combination group conferred 90% protection against the challenge, although there was no statistical difference when compared to both the CpG and AddaVax groups. Interestingly, the weight loss of the AddaVax group was comparable to that of the combination group, while the weights of the CpG group remained consistent and the weight even increased for some mice. Neutralizing antibodies were measured on day 56 using a plaque reduction neutralization test (PRNT), although minimal neutralization was observed across all groups (**Supplementary Figure 7**).

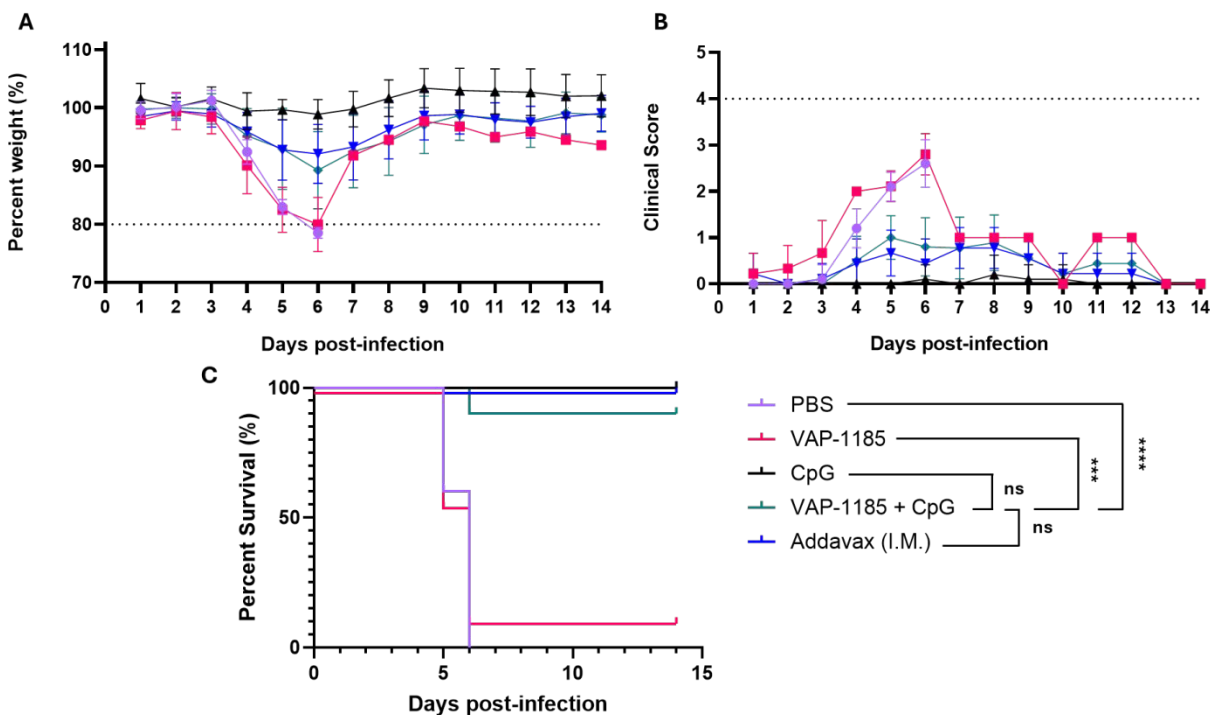


Figure 5. After intranasal vaccination with B5R, mice were challenged with 5×10^4 PFU of vaccinia virus (Western reserve). (A) Body weight measurements normalized to day 0, (B) clinical scores, and (C) survival were evaluated daily for 14 days. Survival was



measured using a Kaplan-Meier survival analysis, with significant differences determined by using a Logrank (Mantel-Cox) test. (ns = not significant; *** $p \leq 0.001$; **** $p \leq 0.001$)

VAP-1185 combined with CpG exhibits a favorable safety profile

While the dual-adjuvant formulation elicited a substantial immune response and provided protection comparable to FDA-approved adjuvants, its overall safety profile also requires evaluation. To establish this, we evaluated nasal cavity tissues and assessed acute liver health following administration of the vaccine. To evaluate whether the vaccine formulation was inducing inflammation in the nasal cavities following administration, histological analysis of the nasal canals was performed. For an intranasal vaccination to stimulate an effective immune response, a mild inflammatory response is desirable, as it can improve antigen presentation and further activate the immune system to respond to the pathogen the vaccine is targeting. However, more severe inflammation can lead to tissue damage, resulting in negative side effects such as pain and irritation.

To evaluate safety, C57BL/6 mice were administered each vaccine formulation I.N., and nasal cavities were harvested 24 hours later for histological analysis. Compared to PBS, mice that received VAP-1185, alone or in combination with CpG, displayed minimal to mild acute rhinitis marked by the presence of neutrophils, macrophages, and protein-rich fluid within the airways and inflammatory cells were occasionally evident within respiratory mucosa. Inflammation was not associated with any epithelial injury microscopically. Mice administered formulations containing CpG alone were comparable to those administered PBS (**Figure 6A-H**) and had no evidence of nasal inflammation. The influx of neutrophils in the groups containing VAP-1185 could be suggestive of VAP-1185 activating MCs, as activated MCs are known to recruit neutrophils.^{32, 33} However,



further studies on the mechanism of this inflammatory cell infiltrate will be required. Additionally, there was individual cell apoptosis/necrosis present in the olfactory epithelium in both the VAP-1185 alone, and in combination with CpG groups, in comparison to PBS, with the CpG group again being comparable to PBS (**Figure 6I-L**). The significance of this finding is uncertain. Based on these results, the VAP-1185 + CpG formulation was found to be locally tolerated without significant adverse effects.

Increases in serum alanine aminotransferase (ALT) are commonly used as a biomarker for liver injury, as this cytosolic hepatocyte enzyme is released into circulation following cell membrane damage or hepatocellular dysfunction.³⁴ Monitoring ALT levels provides a sensitive measure of potential hepatotoxicity in preclinical vaccine studies. In this study, serum ALT levels in all vaccinated groups were not statistically different from those in the PBS control group, indicating that the vaccine formulations did not induce acute liver injury in mice (**Figure 6M**). These findings suggest that both the individual adjuvants and the combination formulation are somewhat well tolerated by the liver. Importantly, the absence of elevated ALT supports the overall safety profile of these formulations, demonstrating that the immunogenic responses observed are unlikely to be confounded by hepatotoxicity. Taken together, these results provide evidence that the vaccine strategy can elicit immune responses without compromising liver integrity, an important consideration for further preclinical development and eventual translational studies.



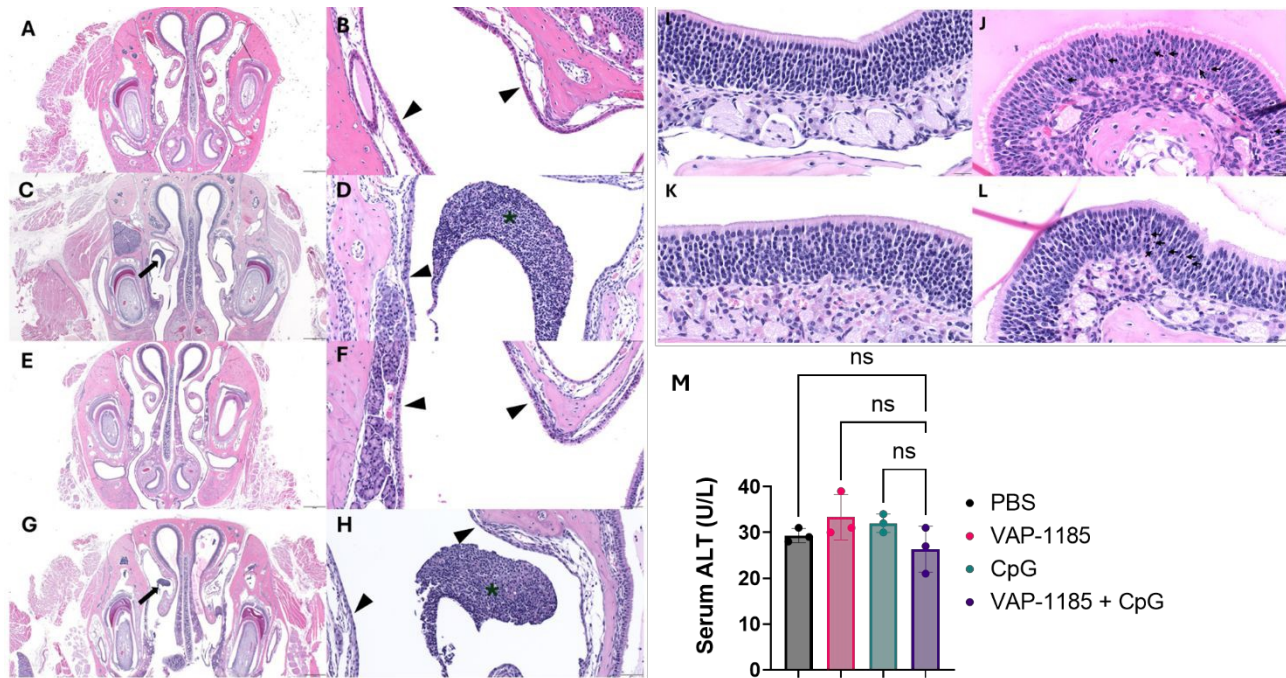


Figure 6. C57BL/6 mice were administered vaccine I.N. and 24 hours later serum and nasal tissues were harvested. Histological sections of the nasal cavity are shown at (A) PBS, 20x magnification, (B) PBS, 200x, (C) VAP-1185, 20x, (D) VAP-1185, 200x, (E) CpG, 20x, (F) CpG, 200x, (G) VAP-1185 + CpG, 20x, (H) VAP-1185 + CpG, 200x. Histological sections of the olfactory epithelium are shown at 400x magnification: (I) PBS, (J) VAP-1185, (K) CpG, and (L) VAP-1185 + CpG. Serum levels of (M) ALT for each group were quantified. Data represented as mean + SD. Significant differences determined by using a one-way ANOVA with Tukey's multiple comparisons (ns = not significant). * denotes immune cell infiltration. Black arrows in A-H indicate respiratory epithelium; arrows in I-L highlight apoptosis/individual cell necrosis.

In summary, after performing extensive SAR analysis we have developed a small molecule MCA that can effectively induce MC degranulation *in vitro*. When combined with the FDA-approved adjuvant, CpG, the two molecules can generate an additive antigen-specific humoral immune response while concurrently producing a cellular response comparable to the Th1-biased CpG. When combined with the vaccinia virus protein antigen, B5R, the dual-adjuvant formulation elicits 90% protection against a lethal challenge of vaccinia virus. Finally, the dual-adjuvant formulation exhibited a favorable safety profile, with unchanged ALT concentrations and only minor acute rhinitis. Therefore, we have developed an effective Th1/Th2 balanced, dual-adjuvant, mucosal



vaccine formulation that may be evaluated in the future against other infectious diseases.

Acknowledgements

Funding for this work was provided by NIH NIAID grant R01AI167099 and NIH NIAID Adjuvant Discovery Contract #HHSN272201400054C for the VAP-1185 SAR. Histopathology/Digital Pathology was performed by the Pathology Services Core at the University of North Carolina-Chapel Hill, which is supported in part by an NCI Center Core Support Grant (P30CA016086). ^1H and ^{13}C NMR characterization was supported by NIH grant S10OD032476 for upgrading the 500 MHz NMR spectrometer in the UNC Eshelman School of Pharmacy NMR Facility. We thank the University of North Carolina's Department of Chemistry Mass Spectrometry Core Laboratory, especially Dr. Brandie Ehrmann, PhD, for their assistance with mass spectrometry analysis, which is based upon work supported by the National Science Foundation under Grant No. CHE-1726291. Blood chemistry was performed by the Animal Clinical Services Core at the University of North Carolina-Chapel Hill. Thank you to Dr. Alexandra Schaefer, PhD for demonstrating how to isolate nasal canals. Additional thanks to Dr. Tom O'Brien, PhD and Tetracore, Inc. for graciously providing an rabbit anti-vaccinia antibody for evaluation.

Supplemental Data

Table S1 contains the 35 analogs of parent compound ST101036 developed after SAR analysis. Figure S1 contains a ^1H -NMR spectrum of VAP-1185. Figure S2 contains a ^{13}C -NMR spectrum of VAP-1185. Figure S3 contains a mass spectrum of VAP-1185. Figure S4 contains a graph showing the TEER over time in RPMI 2650 cells treated with VAP-1185. Figure S5 contains anti-OVA IgG and IgA antibody titers from the NW and BAL of vaccinated mice measured by ELISA. Figure S6 contains IL-2 and IFN- γ ELISpot graphs



with representative images from the splenocytes of vaccinated mice. Figure S7 contains a graph showing the quantity of plaques/well in BS-C-1 cells treated with serum/virus.

Author Contributions Statement

CTM, EMB and KMA designed the experiments. CTM, GLW, LOP, ATH, ESP, and AML performed animal studies. CTM, GLW, LOP, ATH, and AML assisted in tissue harvesting and organ processing. BTJW, HWC, DMG, and SK were involved in SAR analysis. RSS performed histological analysis. JMB performed TEER analysis. CTM and ATH made figures. KMA, EMB, SNA, and HFS supervised experiments. CTM wrote the manuscript with input from all coauthors.

Conflict of Interest

The authors declare that there are no conflicts of interest regarding the publication of this paper.

Data Accessibility

The data supporting this study are publicly available through the ImmPort database (<https://www.immport.org>), in compliance with the NIH Data Management and Sharing Policy promoting open access to federally funded research data. Further details can be accessed upon request.



Works Cited

1. G. Pauli, J. Blümel, R. Burger, C. Drosten, A. Gröner, L. Gürtler, M. Heiden, M. Hildebrandt, B. Jansen and T. Montag-Lessing, *Transfusion Medicine and Hemotherapy*, 2010, **37**, 351.
2. P. Berche, *Presse Med*, 2022, **51**, 104117.
3. C. Maluquer de Motes and D. O. Ulaeto, *Nature medicine*, 2025, 1-4.
4. K. Alibek, *International journal of infectious diseases*, 2004, **8**, 3-8.
5. U. S. F. D. Administration, Key Facts About Vaccines to Prevent Mpox Disease, <https://www.fda.gov/vaccines-blood-biologics/vaccines/key-facts-about-vaccines-prevent-mpox-disease>).
6. Y. C. Ai-ris, K. McMahan, C. Jacob-Dolan, J. Liu, E. N. Borducchi, B. Moss and D. H. Barouch, *JAMA*, 2024, **332**, 1669-1672.
7. B. J. Gowda, M. G. Ahmed and A. Sanjana, *Resonance*, 2022, **27**, 63-85.
8. P. N. Boyaka, *The Journal of Immunology*, 2017, **199**, 9-16.
9. M. Fragoso-Saavedra and M. A. Vega-López, *Journal of Leukocyte Biology*, 2020, **108**, 835-850.
10. J. Lu, H. Xing, C. Wang, M. Tang, C. Wu, F. Ye, L. Yin, Y. Yang, W. Tan and L. Shen, *Signal Transduction and Targeted Therapy*, 2023, **8**, 458.
11. O. Alpan, G. Rudomen and P. Matzinger, *The Journal of Immunology*, 2001, **166**, 4843-4852.
12. Y. Fukuyama, K. Okada, M. Yamaguchi, H. Kiyono, K. Mori and Y. Yuki, *PLoS One*, 2015, **10**, e0139368.
13. C. T. Murphy, E. M. Bachelder and K. M. Ainslie, *International Journal of Pharmaceutics*, 2025, 125300.
14. M. Fong and J. S. Crane, 2018.
15. J. B. McLachlan, C. P. Shelburne, J. P. Hart, S. V. Pizzo, R. Goyal, R. Brooking-Dixon, H. F. Staats and S. N. Abraham, *Nature medicine*, 2008, **14**, 536-541.
16. H. W. Choi, C. Chan, I. D. Shterev, H. E. Lynch, T. J. Robinette, B. T. Johnson-Weaver, J. Shi, G. D. Sempowski, S. Y. Kim and J. K. Dickson, *SLAS DISCOVERY: Advancing Life Sciences R&D*, 2019, **24**, 628-640.
17. D. A. Hendy, B. T. Johnson-Weaver, C. J. Batty, E. M. Bachelder, S. N. Abraham, H. F. Staats and K. M. Ainslie, *International journal of pharmaceutics*, 2023, **634**, 122658.
18. A. Carroll-Portillo, J. L. Cannon, J. Te Riet, A. Holmes, Y. Kawakami, T. Kawakami, A. Cambi and D. S. Lidke, *Journal of Cell Biology*, 2015, **210**, 851-864.
19. T. Zhao, Y. Cai, Y. Jiang, X. He, Y. Wei, Y. Yu and X. Tian, *Signal transduction and targeted therapy*, 2023, **8**, 283.
20. D. Jin and J. Sprent, *The Journal of Immunology*, 2018, **201**, 3129-3139.
21. J. M. A. Bachelder, Kristy M, *ChemRxiv - Analytical Chemistry*, 2025, DOI: <https://doi.org/10.26434/chemrxiv-2025-jtvlk>.
22. B. B. Karakocak, S. Keshavan, G. Gunasingam, S. Angeloni, A. Auderset, A. Petri-Fink and B. Rothen-Rutishauser, *Eur J Pharm Sci*, 2023, **188**, 106511.
23. J. F. Lim, H. Berger and I.-h. Su, *Journal of visualized experiments: JoVE*, 2016, 54596.



24. M. Castells, M. Madden and C. A. Oskeritzian, *Current Allergy and Asthma Reports*, 2025, **25**, 5.
25. M. Zhou, H. Xiao, X. Yang, T. Cheng, L. Yuan and N. Xia, *MedComm (2020)*, 2025, **6**, e70056.
26. C. G. Jones and C. Chen, *Sensors and Actuators A: Physical*, 2020, **314**, 112216.
27. E. Wilms, F. J. Troost, M. Elizalde, B. Winkens, P. de Vos, Z. Mujagic, D. M. Jonkers and A. A. Masclee, *Scientific reports*, 2020, **10**, 475.
28. Y.-Y. C. Mosley, J. E. Radder and H. HogenEsch, *Vaccines*, 2019, **7**, 124.
29. L. F. de Freitas, R. P. Oliveira, M. C. Miranda, R. P. Rocha, E. F. Barbosa-Stancioli, A. M. C. Faria and F. G. da Fonseca, *Journal of virology*, 2019, **93**, 10.1128/jvi. 02191-02118.
30. E. Bell, M. Shamim, J. C. Whitbeck, G. Sfyroera, J. D. Lambris and S. N. Isaacs, *Virology*, 2004, **325**, 425-431.
31. Y. Chu, Y. He, W. Zhai, Y. Huang, C. Tao, Z. Pang, Z. Wang, D. Zhang, H. Li and H. Jia, *International Immunopharmacology*, 2024, **138**, 112593.
32. K. De Filippo, A. Dudeck, M. Hasenberg, E. Nye, N. van Rooijen, K. Hartmann, M. Gunzer, A. Roers and N. Hogg, *Blood, The Journal of the American Society of Hematology*, 2013, **121**, 4930-4937.
33. A. L. Christy, M. E. Walker, M. J. Hessner and M. A. Brown, *Journal of autoimmunity*, 2013, **42**, 50-61.
34. K. Moriles, M. Zubair and S. Azer, *StatPearls*, 2024.



Data Accessibility

The data supporting this study are publicly available through the ImmPort database (<https://www.immport.org>), in compliance with the NIH Data Management and Sharing Policy promoting open access to federally funded research data. Further details can be accessed upon request.

